

# 1 Parton picture of hard scattering processes

This note discusses scattering processes occurring via strong interactions and involving momentum transfers  $Q$  large compared with the QCD scale  $\Lambda_{\text{QCD}} \approx 1 \text{ fermi}^{-1}$ . These are referred to as hard scattering processes. For  $Q \gg \Lambda_{\text{QCD}}$ ,  $\alpha_s(Q) \ll 1$ , and hadrons can be thought of as being made of weakly interacting “partons” (quarks and gluons).

In this regime, the key idea will be to separate dynamics at short distances and dynamics at long distances in the scattering process. The precise way in which this separation is done will differ in different processes. The discussion will treat a few examples, distinguishing observables in which the long-distance physics contributes terms to the physical cross sections that are suppressed by powers of the hard scale  $Q$  (e.g., the cross section for  $e^+e^-$  annihilation into hadrons), and observables in which the long-distance physics contributes already at the leading power in the hard scale  $Q$  (e.g., deep inelastic scattering and hadron-hadron collisions). The former are discussed in the first section, the latter are discussed in the second section.

## 1.1 Infrared-safe processes

In this section we introduce the notion of infrared safety using the example of hadron production in electron-positron annihilation.

### 1.1.1 Hadron production in $e^+e^-$ annihilation

Consider the production of hadrons in electron-positron annihilation at high energy (Fig. 1). The electron pair annihilates into a vector boson (virtual photon or  $Z$ ) with momentum  $q^\mu$  and large  $Q^2 = q^\mu q_\mu$ :

$$\sqrt{Q^2} \gg \text{“hadronic scale”} \approx 1 \text{ fermi}^{-1} \quad . \quad (1)$$

At some point in spacetime, the vector boson decays into a quark and an antiquark. From the uncertainty principle the time of creation of the pair is determined within

$$\delta t \sim 1/\sqrt{Q^2} \ll 1 \text{ fermi} \quad . \quad (2)$$

This quark system evolves in time possibly emitting other quarks and gluons (partons). Over time intervals of the order

$$\Delta t \gg 1/\sqrt{Q^2} \quad (3)$$

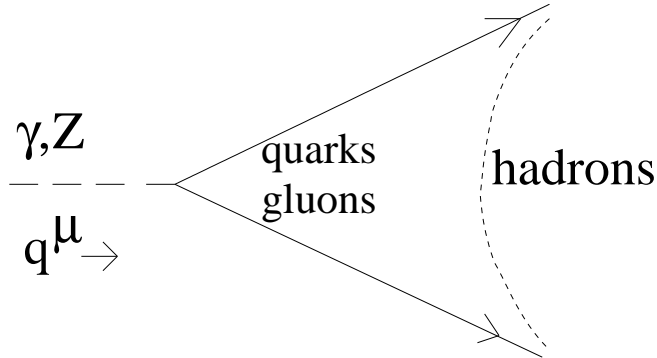


Figure 1: Hadron production from vector boson decay in  $e^+e^-$  annihilation.

the partons convert into hadrons, which are observed in the detectors.

The starting point of our discussion is that the parton process, characterized by the time-scale (2), is calculable from QCD using perturbation theory, while the hadronization process, characterized by the time-scale (3), is not, and is regarded for the purpose of this discussion as “uncalculable”. We rely on the smallness of the coupling in the region (1):

$$\alpha_s(Q) \sim [\beta_0 \ln(Q^2/\Lambda_{\text{QCD}}^2)]^{-1} \quad , \quad \Lambda_{\text{QCD}} \sim 1 \text{ fermi}^{-1} \quad , \quad (4)$$

where  $\beta_0 = (33 - 2N_f)/(12\pi)$ , with  $N_f$  the number of quark flavors. Although the dynamics of hadronization is not known, we however take it to obey general principles such as probability conservation and relativity. Then we ask the question: by using these principles and the part of QCD that we are able to calculate, can we predict the cross section  $\sigma(e^+e^- \rightarrow \text{hadrons})$ ? And, even more strongly, could we predict not just the total cross section but also more detailed features of the hadronic final states?

#### *Separation of short-time and long-time dynamics*

We may examine these questions using a heuristic argument. The process of Fig. 1 consists of a short-distance interaction involving the decay of the vector boson into a parton system and a long-distance interaction converting the parton system into hadrons. The first step in the argument is to declare that as these two interactions occur at different time-scales they have no quantum-mechanical interference: the probability for the whole process can be calculated as a classical product of probabilities for the two subprocesses,

$$P(e^+e^- \rightarrow h) = P(e^+e^- \rightarrow q\bar{q})P(q\bar{q} \rightarrow h) \quad , \quad (5)$$

where  $h$  denotes the hadron final state.

Next we input the completeness of the hadron states. For a given initial state  $|i\rangle$ , the sum of the transition probabilities  $|i\rangle \rightarrow |h\rangle$  over all possible hadron states  $|h\rangle$  equals unity:

$$\sum_h P(i \rightarrow h) = 1 \quad . \quad (6)$$

Then for the total cross section we have

$$\begin{aligned} \sigma_{\text{tot}}(e^+e^- \rightarrow h) &\equiv \sum_h P(e^+e^- \rightarrow h) \\ &= P(e^+e^- \rightarrow q\bar{q}) \sum_h P(q\bar{q} \rightarrow h) = P(e^+e^- \rightarrow q\bar{q}) \quad . \end{aligned} \quad (7)$$

Here we have applied the condition (6) to the long-distance process  $q\bar{q} \rightarrow h$ . We are saying that although we do not know how partons become hadrons, we however know that they always do.

The formula (7) begins to show a structure of the kind we would like to have: on the left hand side is a hadronic quantity — that is, measurable; on the right hand side is a partonic quantity — that is, “calculable”. However, we haven’t quite arrived at what we wanted yet: indeed, if we tried to calculate the right hand side of Eq. (7) in perturbation theory, we would find a divergent result. As we will see shortly, the divergence arises from residual long-time effects. But there is a natural solution for this, which comes about since we need to account for the nonconservation of particle number in relativistic field theory. This means that we need to account for all possible multiparticle final states. For instance, at the first order of perturbation theory we need to add in the contribution of states  $q\bar{q}g$ .

Let us then see what happens. Suppose we computed  $\sigma(e^+e^- \rightarrow q\bar{q})$  in perturbation theory with a time cut-off  $t < T$ . We can think of implementing this, for instance, by introducing a gluon mass  $m_g$ ,  $T \sim m_g^{-1}$ . The result we find at the first order in the coupling  $\alpha_s$  is of the form

$$\begin{aligned} \sigma(e^+e^- \rightarrow q\bar{q}) &= \sigma_0 \{ 1 + \alpha_s [ -a_2 \ln^2(T\sqrt{Q^2}) + a_1 \ln(T\sqrt{Q^2}) \\ &\quad + \text{finite terms for } T \rightarrow \infty ] + \mathcal{O}(\alpha_s^2) \} \quad , \end{aligned} \quad (8)$$

where  $\sigma_0$  is the pointlike cross section given by the Born approximation, and  $a_1$  and  $a_2$  are numerical coefficients. Eq. (8) diverges, as advertised above, as we let the cut-off  $T$  go to  $\infty$ . If we now calculate the  $q\bar{q}g$  contribution with the same method, we find

$$\begin{aligned} \sigma(e^+e^- \rightarrow q\bar{q}g) &= \sigma_0 \alpha_s [ a_2 \ln^2(T\sqrt{Q^2}) - a_1 \ln(T\sqrt{Q^2}) \\ &\quad + \text{finite terms for } T \rightarrow \infty ] + \mathcal{O}(\alpha_s^2) \quad . \end{aligned} \quad (9)$$

The divergent dependence on  $T$ , parameterizing the effects of long-time physics, cancels in the sum of (8) and (9). What does this mean? As  $T$  increases, the probability of

having a  $q\bar{q}g$  state increases, while the probability of having a  $q\bar{q}$  state decreases. But the total cross section is insensitive to this, i.e., to details of the long-time interactions. It can be shown that this independence of long-time dynamics is not a characteristic of the first-order calculation only, but it holds true for any order in  $\alpha_s$ . Thus  $\sigma_{\text{tot}}$  can be legitimately evaluated as a systematic expansion in perturbation theory. The result is known through the third order:

$$\sigma_{\text{tot}}(e^+e^- \rightarrow h) = \sigma_0 \left[ 1 + \frac{\alpha_s}{\pi} + 1.4092 \left( \frac{\alpha_s}{\pi} \right)^2 - 12.805 \left( \frac{\alpha_s}{\pi} \right)^3 + \dots \right] , \quad (10)$$

where  $\alpha_s$  is the strong coupling evaluated at the scale  $Q$ .

The insensitivity to long-time dynamics that we have just observed is referred to as infrared safety. Importantly, this property holds for many other observables besides the total cross section. We will come back to this.

#### *Renormalization group invariance*

Short-time fluctuations are incorporated in the cross section through the dependence of the coupling on the energy scale. This follows from the renormalization of the theory,

$$\alpha_s(\mu) = \frac{\alpha_s(\mu')}{1 + \beta_0 \alpha_s(\mu') \ln(\mu^2/\mu'^2)} , \quad (11)$$

with  $\beta_0$  given below Eq. (4). Note the implications of this on the structure of the answer for  $\sigma$ . We have written Eq. (10) as an expansion in powers of  $\alpha_s = \alpha_s(Q)$ . If the scale is changed from  $Q$  to an arbitrary scale  $\mu$ , at one-loop accuracy the coupling is changed to

$$\alpha_s \rightarrow \alpha_s(\mu) = \frac{\alpha_s}{1 + \beta_0 \alpha_s \ln(\mu^2/Q^2)} = \alpha_s - \beta_0 \alpha_s^2 \ln(\mu^2/Q^2) + \mathcal{O}(\alpha_s^3) , \quad (12)$$

and the perturbative expansion for the cross section takes the form

$$\begin{aligned} \sigma_{\text{tot}} &= \sigma_0 \left\{ 1 + [c_1 + c'_1 \ln(\mu^2/Q^2)] \alpha_s(\mu) \right. \\ &\quad \left. + [c_2 + c'_2 \ln(\mu^2/Q^2) + c''_2 \ln^2(\mu^2/Q^2)] \alpha_s^2(\mu) + \mathcal{O}(\alpha_s^3) \right\} , \end{aligned} \quad (13)$$

where the  $c$ 's are numerical coefficients. But the invariance of the physical cross section under changes in the renormalization scale requires that, order by order in  $\alpha_s$ ,

$$\sigma(\alpha_s(\mu), \mu/Q) = \sigma(\alpha_s, 1) . \quad (14)$$

Via Eq. (14), the coefficients of the logarithmic terms in Eq. (13) are uniquely determined in terms of the non-logarithmic coefficients, given in Eq. (10), and the running of the coupling (12). For example, to second order Eq. (14) implies  $c'_1 = c''_2 = 0$ ,  $c'_2 = c_1 \beta_0$ . This represents a powerful, simple consequence of renormalization-group invariance. We will see other applications of this invariance in the next section.

### 1.1.2 Final-state observables

If all we could compute in the approach discussed above was the total cross section, the results would be very limited. The point is that in fact many detailed features of the hadronic final states are describable through infrared-safe observables.

To distinguish between observables that are infrared safe and observables that aren't, one can give simple general criteria. For interactions among partons to occur at large times and distances, small relative momenta are required. This means that either we have two partons moving in almost the same direction (collinear configurations, Fig. 2a) or all components of a parton momentum are small (soft configurations, Fig. 2b). Then an observable will be infrared-safe if it is left unchanged by a) partons splitting into collinear partons and b) partons emitting soft gluons.

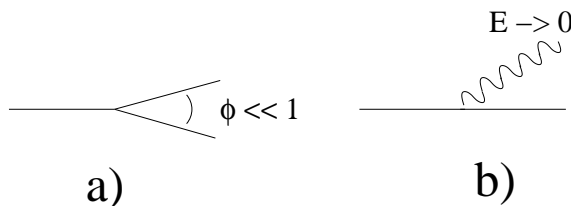


Figure 2: Collinear and soft parton emission.

#### *Criteria for infrared safety*

To state this precisely, parameterize the generic observable  $\Sigma$  in terms of  $n$ -particle differential cross sections  $\sigma_n$  and weight functions  $W_n^{(\Sigma)}$  of the  $n$  final-state momenta  $p_1, \dots, p_n$ , as follows:

$$\Sigma = \sum_n \frac{1}{n!} \int [dp_i] \frac{d\sigma_n}{dp_1 \dots dp_n} W_n^{(\Sigma)}(p_1, \dots, p_n) \quad , \quad (15)$$

where  $[dp_i]$  denotes the integration over the final-state phase space, and  $W_n$  can be taken to be symmetric functions of their arguments. Then infrared safety for the observable  $\Sigma$  means that

$$W_{n+1}^{(\Sigma)}(p_1, \dots, \lambda p_n, (1 - \lambda)p_n) = W_n^{(\Sigma)}(p_1, \dots, p_n) \quad , \quad 0 \leq \lambda \leq 1 \quad . \quad (16)$$

That is, the weight functions  $W^{(\Sigma)}$  are left unchanged if one particle splits into two collinear particles ( $0 < \lambda < 1$ ) or emits a soft particle ( $\lambda \rightarrow 0, 1$ ).

The case of the total cross section that we have seen before,  $\Sigma = \sigma_{\text{tot}}$ , is the case  $W = 1$ . Another well-known example of an infrared-safe quantity is the correlation between the energies that flow into two detectors separated by an angle  $\theta$ , defined by

$$W = \frac{1}{Q^2} \sum_{i,j} E_i E_j \delta(\cos \theta_{ij} - \cos \theta) \quad . \quad (17)$$

To verify Eq. (16) for the energy-energy correlation, observe that the contribution from a particle with  $E \rightarrow 0$  vanishes, and that collinear splitting does not change  $W$ , since the autocorrelation terms give

$$\lambda^2 E_n^2 + 2\lambda(1-\lambda)E_n^2 + (1-\lambda)^2 E_n^2 = E_n^2 \quad (18)$$

and the crossed terms give

$$\lambda E_n E_i + (1-\lambda)E_n E_i = E_n E_i \quad . \quad (19)$$

The best-known illustration of the concept of infrared safety is provided by the physics of hadronic jets. We consider these next.

### *Jets*

Hadronic jets are, roughly speaking, sprays of particles going in approximately the same direction. The clustering of particles into what we call a jet can be defined in a precise manner through algorithms that satisfy the criteria for infrared safety. It is this property that allows precision phenomenology, including measurements of the QCD coupling  $\alpha_s$ , to be done in experiments on jet physics.

The earliest infrared-safe definition of jets is that of Fig. 3. According to this definition, the hadronic event of Fig. 3 contributes to the jet cross section if, given  $\varepsilon > 0$ , there exist two cones of opening angle  $\delta$  such that the energy  $E_{\text{out}}$  going outside the cones is smaller than a fraction  $\varepsilon$  of the total energy  $E$ .

Let us check explicitly at the leading level that this definition is infrared-safe. To this end note that the jet cross section receives contribution at order  $\alpha_s$  by the emission of a virtual gluon, by the emission of a real gluon with energy  $< \varepsilon E$ , and by the emission of a real gluon with energy  $> \varepsilon E$  and direction within the cones  $\delta$ . We now take the divergent parts — soft ( $\omega \rightarrow 0$ ) and collinear ( $\theta \rightarrow 0$ ) — for each of these contributions, and add them up. We find

$$\begin{aligned} \sigma^{(\text{jet})}(\varepsilon, \delta) &= \sigma_0 \left\{ 1 + 2 \frac{\alpha_s}{\pi} C_F \left[ - \int_0^E \frac{d\omega}{\omega} \int_0^\pi \frac{d \cos \theta}{1 - \cos^2 \theta} + \int_0^{\varepsilon E} \frac{d\omega}{\omega} \int_0^\pi \frac{d \cos \theta}{1 - \cos^2 \theta} \right. \right. \\ &\quad \left. \left. + \int_{\varepsilon E}^E \frac{d\omega}{\omega} \left( \int_0^\delta \frac{d \cos \theta}{1 - \cos^2 \theta} + \int_{\pi-\delta}^\pi \frac{d \cos \theta}{1 - \cos^2 \theta} \right) \right] \right\} \quad (20) \end{aligned}$$

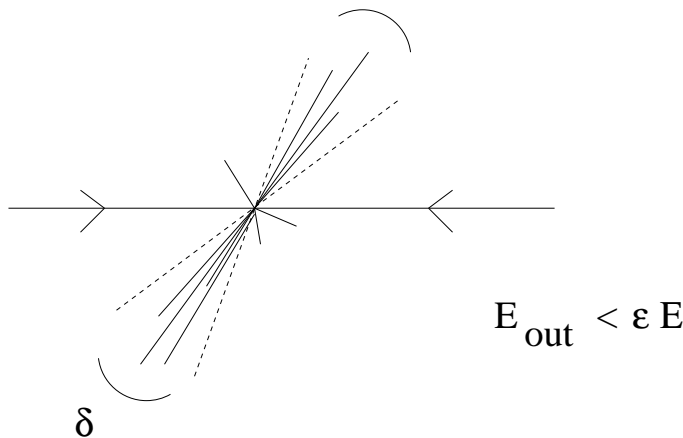


Figure 3: Jet cones.

The contribution of real gluon emission with energy below  $\varepsilon E$  is cancelled entirely by the corresponding virtual emission. The real contribution above  $\varepsilon E$  within the cones  $\delta$  is also cancelled by the virtuals, leaving

$$\sigma^{(\text{jet})}(\varepsilon, \delta) = \sigma_0 \left\{ 1 - 2 \frac{\alpha_s}{\pi} C_F \int_{\varepsilon E}^E \frac{d\omega}{\omega} \int_{\delta}^{\pi-\delta} \frac{d \cos \theta}{1 - \cos^2 \theta} \right\} \simeq \sigma_0 \left\{ 1 - 4 \frac{\alpha_s}{\pi} C_F \ln \varepsilon \ln \delta \right\} \quad , \quad (21)$$

which is finite for any finite  $\varepsilon, \delta$ . The logarithmic enhancements for small  $\varepsilon, \delta$  are an example of soft/collinear effects that call for calculational techniques beyond the fixed order in  $\alpha_s$ . We will talk of this in Sec. 2.3.

Current experiments do not rely on the simple definition above for identifying jets but use more sophisticated procedures based on clustering algorithms. In addition to jet cross sections, a variety of shape variables describing more detailed features of the events can also be introduced in an infrared-safe manner. Measurements of hadronic jet rates and event shapes have provided us with precise determinations of the QCD coupling  $\alpha_s$ .

### 1.1.3 Beyond the $\alpha_s$ expansion

For sufficiently large  $Q^2$  we have been able to relate hadronic observables to partonic calculations. We now want to look more closely at the arguments that have led us to this parton-hadron correspondence. The discussion brings us to issues that go beyond the expansion in  $\alpha_s$ , and help us parameterize the structure of the corrections to it.

We have assumed that at large  $Q^2$  many hadron states are available for partons to

convert to, and we have used the completeness of the hadron states to get a relation between parton-level and hadron-level quantities. When  $Q^2$  approaches the thresholds of hadron resonances, though, we don't expect a perturbative partonic calculation to be able to describe the complex structure of the hadronic cross section. Nevertheless, it can be shown that less strong relations apply, which connect integrals of the hadronic cross section over large energy regions to correlation functions of quark operators calculable at short distances.

To see how these relations come about, we start with implementing probability conservation by applying the optical theorem to the total cross section for  $e^+e^- \rightarrow$  hadrons (Fig. 4). This relates  $\sigma_{\text{tot}}$  to the imaginary part of the correlator of two electromagnetic currents,

$$\sigma_{\text{tot}}(Q^2) = \frac{4\pi\alpha}{Q^2} \text{Im}\Pi(Q^2) \quad , \quad (22)$$

with

$$i \int d^4x e^{iq \cdot x} \langle 0 | T(j_\mu(x) j_\nu(0)) | 0 \rangle = (q^\mu q^\nu - Q^2 g^{\mu\nu}) \Pi(Q^2) \quad . \quad (23)$$

Eqs. (22),(23) relate the hadronic cross section to a correlator of quark operators, which does not contain any explicit dependence on specific hadron states. But we still do not know how to calculate this correlator, since for large, timelike  $Q^2$  the integral (23) receives contributions from energetic intermediate states with multiple hadrons propagating to long times and distances.

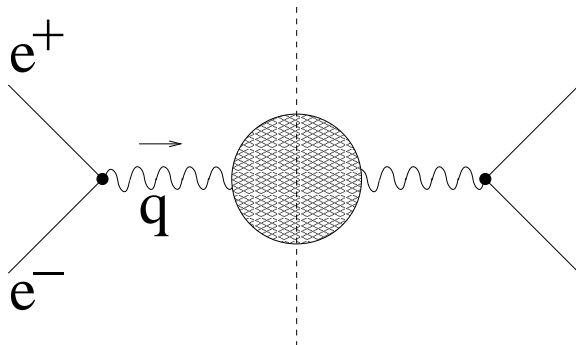


Figure 4: Optical theorem for the hadronic cross section.

We circumvent this by appealing to the analyticity properties of  $\Pi$ . Relativistic causality implies that  $\Pi$  must be an analytic function in the complex  $Q^2$  plane, with a branch cut on the positive axis from the lowest hadronic threshold to infinity. Then we can write a dispersion relation in the following way. Take a large, negative value of virtuality



$Q^2 = -Q_0^2$ , and consider the following integral along a contour encircling  $-Q_0^2$ :

$$\oint_C \frac{dQ^2}{2\pi i} \frac{\Pi(Q^2)}{(Q^2 + Q_0^2)^{n+1}} \quad , \quad n \geq 1 \quad . \quad (24)$$

We can first evaluate this integral on a small circle around  $-Q_0^2$  using the residues' theorem. The result is proportional to the  $n$ th derivative of  $\Pi$ . Next we can deform the contour as in Fig. 5. The contour at infinity does not contribute for  $n \geq 1$ , and we are left with the discontinuity of  $\Pi$  across the cut. This is proportional to  $\text{Im } \Pi$  and related to  $\sigma_{\text{tot}}$  via Eq. (22). By equating the results from the two contour integrals we obtain a set of relations, or sum rules, between derivatives of  $\Pi$  at  $-Q_0^2$  and integrals over energy of the hadronic cross section:

$$4\pi^2\alpha \frac{1}{n!} \frac{d^n \Pi}{d(Q^2)^n}(-Q_0^2) = \int_{\text{thres.}}^{\infty} dQ^2 \frac{Q^2}{(Q^2 + Q_0^2)^{n+1}} \sigma_{\text{tot}}(Q^2) \quad . \quad (25)$$

The integral on the right hand side of Eq. (25) goes from the lowest hadron threshold to infinity, and the correlator on the left hand side is evaluated at large spacelike  $Q^2 = -Q_0^2$ . At such  $Q^2$  the intermediate states contributing to the integral (23) cannot propagate far from the interaction points, so that a short-distance calculation is valid.

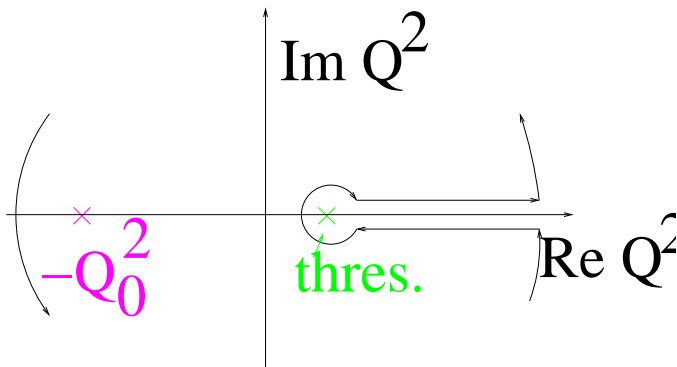


Figure 5: The integration contour in the complex  $Q^2$  plane.

The basic method of doing the calculation is by expanding the product of currents (23) at small distances in a series of local operators,

$$j(x)j(0) = c^{(\mathbf{1})}(x)\mathbf{1} + c^{(qq)}(x)m\bar{q}q(0) + c^{(F^2)}(x)F_{\mu\nu}F^{\mu\nu}(0) + \dots \quad . \quad (26)$$

Here  $\mathbf{1}$ ,  $\bar{q}q$ ,  $F^2$ ,  $\dots$  are gauge-invariant and Lorentz-invariant operators placed at  $x = 0$ , while the perturbatively calculable coefficients  $c$  are c-number functions of  $x$ , containing singularities for  $x \rightarrow 0$ . By dimensional counting,  $c^{(\mathbf{1})}(x) \sim 1/x^6$ ,  $c^{(qq)}(x) \sim 1/x^2$ ,

$c^{(F^2)}(x) \sim 1/x^2$ . Further terms in the expansion (26) come from higher-dimensional operators and are less singular for  $x \rightarrow 0$ .

The expansion (26) tells us about the structure of the corrections to  $\sigma_{\text{tot}}$ . Fourier-transforming the expansion term by term and using Eqs. (22),(23) gives

$$Q^2 \sigma_{\text{tot}}(Q^2) = C^{(\mathbf{1})}(Q^2) + C^{(qq)}(Q^2) \langle 0 | m \bar{q} q | 0 \rangle + C^{(F^2)}(Q^2) \langle 0 | F^2 | 0 \rangle + \dots \quad , \quad (27)$$

where  $C^{(\mathbf{1})} \sim (Q^2)^0$ ,  $C^{(qq)} \sim (Q^2)^{-2}$ ,  $C^{(F^2)} \sim (Q^2)^{-2}$ . Less singular terms in  $x$  give rise to power-suppressed terms in  $1/Q^2$ . The first contribution on the right hand side of Eq. (27) can be identified as the perturbative expansion in powers of  $\alpha_s$ , that is, powers of  $1/\ln Q^2$ . Possible nonperturbative corrections are given by an expansion in powers of  $1/Q^2$ , and contain vacuum expectation values of gauge-invariant local operators, or vacuum condensates.

The vacuum condensates are universal nonperturbative parameters, while the coefficients in front of them can be calculated perturbatively for a given observable. Even though we cannot compute the matrix elements in Eq. (27), from the expansion itself we learn the order of the power correction. In the example above there is no  $1/Q^2$  correction, because there are no gauge-invariant operators of dimension 2 in the expansion (26). The first correction to  $\sigma_{\text{tot}}$  is of order  $1/Q^4$ .

We conclude this subsection by noting that the method to obtain the dispersion sum rules (25) illustrates a potential source of uncertainty of the theoretical predictions. The method involves going to the unphysical  $Q^2$  region, corresponding to imaginary energies. Perturbative calculations are done in this region. The point is that the analytic continuation in the  $Q^2$  plane may itself cause a loss of theoretical accuracy. For instance, an error of order  $\exp(-\sqrt{-Q^2})$  in the perturbative approximation, negligibly small at large negative  $Q^2$ , is turned to  $\sin \sqrt{Q^2}$ , oscillating and unsuppressed. Note that our theoretical prediction will be affected by an error not just because of limitations in calculational capabilities, but because of intrinsic limits on the accuracy of both the  $\alpha_s$  series and the condensate series. The possibility of such effects has been discussed, including violations of parton-hadron duality and possible phenomenological implications.

## 1.2 Factorization and evolution

In this section we go beyond the notion of infrared safety and treat broader classes of processes including hadron scattering.

Consider deep-inelastic electron-proton scattering (DIS), depicted in Fig. 6. The proton has momentum  $p$ , the virtual photon exchanged by the electron has momentum  $q$ ,

and its space-like virtuality is

$$q^\mu q_\mu = -Q^2 \quad , \quad (28)$$

with  $\sqrt{Q^2} \gg 1 \text{ fermi}^{-1}$  being the hard scale. Let  $x$  be the ratio

$$x = \frac{Q^2}{2p \cdot q} \quad . \quad (29)$$

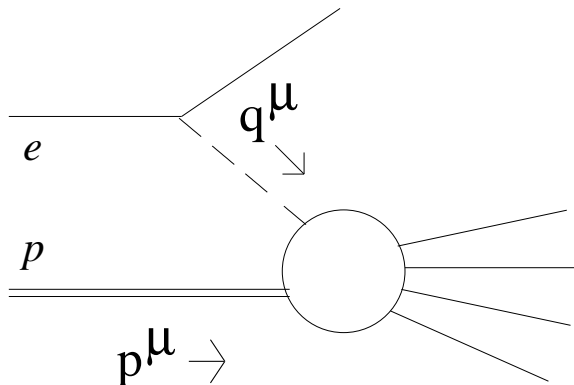


Figure 6: Deep-inelastic lepton-hadron scattering.

In this process, even though the virtual photon couples to quarks over short times of the order of  $1/\sqrt{Q^2} \ll 1 \text{ fermi}$ , the quark wave function has had a long time to develop, as quarks have existed in the proton since times far in the past: the process is necessarily sensitive to long-time interactions, and the arguments of the previous section on infrared safety cannot apply.

### 1.2.1 Factorization in deep inelastic scattering

Although the presence of the hadron observed in the initial state prevents us from disposing of long-time effects simply by means of a unitarity condition, we can nevertheless ask whether long-time effects can be separated out and *factorized*. Considering the physical cross section  $\sigma$ , as a function of the hard momentum scales of order  $Q$  and the soft momentum scales of order the hadronic mass scale  $m$ , we ask whether  $\sigma$  can be expressed as

$$\sigma(Q, m) = C(Q, \text{parton momenta} > \mu) \otimes f(\text{parton momenta} < \mu, m) \quad , \quad (30)$$

that is, as a product (or, in general, a convolution  $\otimes$  whose precise definition is to be specified) of a factor  $C$  that only depends on hard momenta and a factor  $f$  that only

depends on soft momenta, at the price of introducing an auxiliary mass scale  $\mu$  to define the separation of hard and soft.

If such a representation exists, this brings several benefits. First, the  $Q$  dependence of the physical observable becomes computable in perturbation theory, since it is entirely contained in the factor  $C$ , which depends on short-distance physics. Second, although the function  $f$  depends on long distances and is thus not computable, its  $\mu$  dependence is, however, computable: this is because it has to be equal and opposite to that of the function  $C$  in order for the left hand side of Eq. (30) to be independent of  $\mu$ . This invariance of the physical cross section with respect to changes in the scale  $\mu$  can be expressed through renormalization group equations. It can be shown that by dimensional arguments the factor  $C$  will depend on  $\mu$  only through the ratio  $Q/\mu$ . Then from the renormalization group analysis of the  $\mu$  behavior one can learn about the behavior in the physical scale  $Q$ .

Let us consider the scattering of Fig. 6 in a reference frame in which the incoming proton has very large momentum in the  $z$  direction (“infinite-momentum” frame). What happens is depicted in Fig. 7.

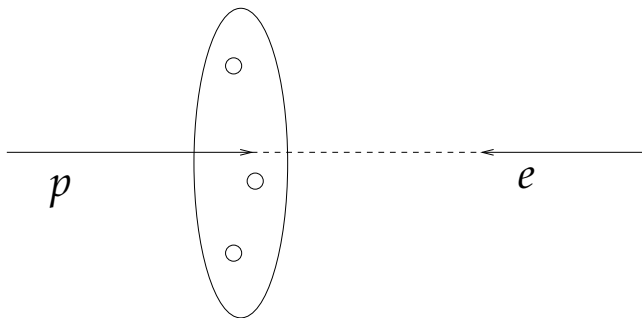


Figure 7: The scattering in the infinite momentum frame.

The proton is Lorentz-contracted in the longitudinal direction. The time it takes the electron to cross the proton,  $\Delta t_{\text{scatter}}$ , shortens as the proton momentum becomes large. On the other hand, the proton’s internal interactions are time-dilated. The typical timescale for parton interactions inside the proton,  $\tau_{\text{parton}}$ , becomes larger and larger as the proton momentum increases. For

$$\Delta t_{\text{scatter}} \ll \tau_{\text{parton}} \quad (31)$$

the electron sees a hadronic state with definite number of partons, each of which is in a state of definite momentum, characterized by a fraction  $\xi$  of the proton’s momentum  $p$ .

For large  $Q^2$  the distance traveled by the virtual photon is small,

$$\Delta l_\gamma \sim 1/\sqrt{Q^2} \ll 1 \text{ fermi} \quad . \quad (32)$$

So if the density of partons is low enough the photon interacts with only one parton. The probability of its interacting with  $n$  partons is suppressed by a factor  $(R_p^2 Q^2)^{-n}$ , where  $R_p$  is the proton radius, and we regard the process as dominated by single parton scattering.

Now, as the photon-parton scattering does not interfere with the interactions among partons occurring at time-dilated scales, by an argument similar to that used in Sec. 1 for final-state interactions we may compute the process by combining probabilities rather than amplitudes. In this situation the cross section is obtainable, up to corrections down by powers of  $Q^2$ , from the (hard) cross section  $\sigma_{e-i}$  for the scattering of the electron from parton  $i$ , carrying momentum fraction  $\xi$  of the proton momentum, times the (soft) distribution function  $f_{i/p}$  of parton  $i$  in the proton:

$$\sigma_{e-p}\left(\frac{Q^2}{2p \cdot q}, Q, m\right) = \sum_i \int_x^1 d\xi \sigma_{e-i}\left(\frac{Q^2}{2\xi p \cdot q}, Q, \mu\right) f_{i/p}(\xi, \mu, m) \left[1 + \mathcal{O}\left(\frac{\Lambda_{\text{QCD}}^2}{Q^2}\right)\right]. \quad (33)$$

Here the sum over partons and integration over  $\xi$  specify the convolution  $\otimes$  of Eq. (30). As a result of the separation of hard and soft contributions, both factors in Eq. (33) now contain an additional mass scale  $\mu$ . Notice here the difference compared to the infrared-safe  $e^+e^-$  cross section of Sec. 1. From this point of view,  $\mu$  is a left-over of the process' sensitivity to long-time interactions.

If we ignore the  $\mu$  dependence, Eq. (33) can be used at the lowest order of perturbation theory, and gives scaling of the cross section in  $1/Q^2$ , reflecting the pointlike nature of the constituents. This is the original parton model of Bjorken and Feynman. In general, Eq. (33) is valid to any perturbative order, and small, logarithmic violations of scaling appear through the  $\mu$  dependence of  $f_{i/p}$  and  $Q/\mu$  dependence of  $\sigma_{e-i}$ . This is the distinctive feature of the field-theoretic treatment of the scattering in QCD, beyond the original parton model.

We have introduced  $\mu$  in Eq. (30) as a momentum cut-off. In more detailed treatments, it will be equivalently introduced by different methods, such as for instance the dimensional regularization method, better-suited for higher-order perturbative calculations.

As there is no interference between different partons and different  $\xi$ , the  $f$  are independent of the hard scattering (“universal”) and can be characterized as matrix elements of the fundamental fields of the theory, representing the partons that connect the incoming hadron with the hard scattering. Denoting by  $p^+$  the hadron's momentum in the lightcone plus direction, the matrix element for the case of the gluon distribution  $i = g$  is

$$f_{g/p}(\xi, \mu) = \frac{1}{2\pi\xi p^+} \int dy^- e^{i\xi p^+ y^-} \langle p | \tilde{F}_a^{+j}(0, 0, \mathbf{0}) \tilde{F}_a^{+j}(0, y^-, \mathbf{0}) | p \rangle, \quad (34)$$

where  $\tilde{F}$  is the gluon field strength  $F$  multiplied by a path-ordered exponential of the color potential,

$$\tilde{F}_a^{+j}(y) = \left[ \mathcal{P} \exp \left( -ig \int_{y^-}^{\infty} dz^- A_c^+(y^+, z^-, \mathbf{y}) t_c \right) \right]_{ab} F_b^{+j}(y) . \quad (35)$$

Eq. (34) may be understood starting from the theory canonically quantized on planes  $x^+ = \text{const.}$  in  $A^+ = 0$  gauge. In this gauge the operator in Eq. (34) can be related to the number operator. In general, though, the definition in Eq. (34) is gauge-invariant: it is made gauge-invariant by the path-ordered exponential (35). This factor has a physical interpretation in terms of the recoil color flow, represented as a fast moving color charge that goes out along a lightlike line in the minus direction, coupling to gluons from the hadron's field. The operator product in Eq. (34) gives rise to ultraviolet divergences that need renormalization. From the point of view of Eq. (34), the dependence on  $\mu$  in the  $f$  appears precisely through the renormalization scale that has to be introduced to treat these divergences.

An expression analogous to (34) can be given for quarks:

$$f_{q/p}(\xi, \mu) = \frac{1}{4\pi} \int dy^- e^{i\xi p^+ y^-} \langle p | \tilde{q}(0) \gamma^+ \tilde{q}(0, y^-, \mathbf{0}) | p \rangle , \quad (36)$$

where

$$\tilde{q}_i(y) = \left[ \mathcal{P} \exp \left( -ig \int_{y^-}^{\infty} dz^- A_c^+(y^+, z^-, \mathbf{y}) t_c \right) \right]_{ij} q_j(y) . \quad (37)$$

The operators in Eqs. (34),(36) are not local. But if we take moments, defined as the Mellin transform

$$f_N(\mu) = \int_0^1 d\xi \xi^{N-1} f(\xi, \mu) , \quad (38)$$

we can verify that these are related to local operators, and establish a connection between Eq. (33) and an expansion of the kind seen in Sec. 1 for the  $e^+e^-$  cross section, Eq. (27). More precisely, the moments (38) of the gluon distribution (34) are expressed in terms of an infinite set of local operators,

$$O^{\mu_1 \dots \mu_N} = F_\nu^{\mu_1}(0) \left( \prod_{j=2}^{N-1} D^{\mu_j} \right) F^{\nu \mu_N}(0) , \quad (39)$$

whose dimensions increase with the moment variable  $N$ ,  $d = 2 + N$ . This infinite set of operators, along with the analogous set for the quark fields, controls the large- $Q^2$  behavior of the cross section at leading power, and represents the operator content of the convolution in Eq. (33), taken to all perturbative orders. This is the counterpart, for deep inelastic scattering, of the first term in the right hand side of the expansion (27) for  $e^+e^-$ . The twist variable  $\tau$  defined as  $\tau \equiv d - N$  takes the value  $\tau = 2$  for the leading-power

operators. Further terms in the local-operator expansion correspond to the contributions  $\mathcal{O}(1/Q^2)$  in Eq. (33), and contain operators with  $\tau = d - N > 2$ .

The factorization of the type (33) can be written for any hard-scattering observable depending on a hard mass scale  $Q^2$ . For instance, let us parameterize the DIS cross section  $\sigma$ , based on Lorentz and gauge invariance, in terms of dimensionless structure functions  $F_T, F_L$  for transversely and longitudinally polarized virtual photons,

$$\frac{d\sigma}{dx dQ^2} = \frac{4\pi\alpha^2}{xQ^4} \left[ \left(1 - y + \frac{y^2}{2}\right) F_2(x, Q^2) - \frac{y^2}{2} F_L(x, Q^2) \right] , \quad (40)$$

where  $F_2$  is given by the combination

$$F_2 = F_L + F_T \quad (41)$$

and

$$y = \frac{Q^2}{xs} , \quad (42)$$

with  $s$  the center-of-mass energy. Any of the  $F_n$  ( $n = 2, L$ ) in Eq. (40) obeys the factorization formula

$$F_n(x, Q) = \sum_i \int_x^1 d\xi C_{ni}(x/\xi, \alpha_s(\mu), Q/\mu) f_i(\xi, \mu) + \mathcal{O}(\Lambda_{\text{QCD}}^2/Q^2) , \quad (43)$$

with  $f$  universal parton distributions and  $C$  process-dependent coefficient functions, computable in perturbation theory as power series expansions in  $\alpha_s$ ,

$$C_{ni}(x, \alpha_s, Q/\mu) = \sum_k C_{ni}^{(k)}(x, Q/\mu) \alpha_s^k . \quad (44)$$

The  $x$  dependence of Eq. (43) can be diagonalized by taking  $N$ -moments for any function of  $x$  as in Eq. (38). Formulas analogous to (43) can be written for a dimensionless cross section  $F(x, Q^2) = Q^2\sigma$ .

In practical applications of Eq. (43), setting the factorization scale  $\mu$  at a value of the order of the hard scale  $Q$  means that potentially large logarithmic corrections in the ratio  $Q/\mu$  are automatically taken into account, or “resummed”, rather than appearing in the perturbative expansions (44) of the hard-scattering coefficient functions at any order.

### 1.2.2 Evolution equations

The important point is that the invariance of the physical observable  $F$  under changes in  $\mu$  implies evolution equations for  $f$ . Schematically, the structure of the equations is as

follows. Since the left hand side of Eq. (43) does not depend on  $\mu$ , we have

$$\frac{d}{d \ln \mu} F_N(Q^2) = 0 \quad . \quad (45)$$

Then  $f$  and  $C$  must obey the equations

$$\frac{d}{d \ln \mu} \ln f_N = \gamma_N = -\frac{d}{d \ln \mu} \ln C_N \quad , \quad (46)$$

with  $\gamma_N$  a function of  $\alpha_s$ , computable as a perturbation expansion

$$\gamma_N(\alpha_s) = \sum_{k=1}^{\infty} b_N^{(k)} \alpha_s^k \quad . \quad (47)$$

So although  $f$ , which depends on soft momentum scales, is not calculable perturbatively, its variation with the scale  $\mu$  is. This result is of great importance, as it allows us to connect the outcomes of experiments at different scales of momentum transfer. From Eq. (46) we get

$$f_N(\mu) = f_N(\mu_0) \exp \left( \int_{\mu_0}^{\mu} \gamma_N(\alpha_s(\mu')) \frac{d\mu'}{\mu'} \right) \quad . \quad (48)$$

The exponential factor in Eq. (48) represents the violation of scaling, governed by the anomalous dimension  $\gamma$ . Inserting in Eq. (48) the expression (4) for the running coupling and the  $\alpha_s$ -dependence (47) of  $\gamma$ , we see that the violation of scaling is logarithmic. Note that if  $\alpha_s$  was frozen to a constant or run to a finite value, this violation would be power-like.

We have written Eqs. (46),(47) in moment space, suppressing parton indices. Transforming back to  $x$  space and restoring the parton indices, the evolution equations read

$$\frac{d}{d \ln \mu^2} f_i(x, \mu) = \sum_j \int_x^1 \frac{d\xi}{\xi} P_{ij}(\alpha_s(\mu), x/\xi) f_j(\xi, \mu) \quad , \quad (49)$$

where  $P_{ij}(\alpha_s, z)$  are the generalized Dokshitzer-Gribov-Lipatov-Altarelli-Parisi (DGLAP) splitting functions, related to the anomalous dimensions  $\gamma_{ij,N}(\alpha_s)$  by the Mellin transform

$$\gamma_{ij,N}(\alpha_s) \equiv \int_0^1 dz z^{N-1} P_{ij}(\alpha_s, z) \quad . \quad (50)$$

It is often useful to also introduce the momentum weighted parton distributions  $\tilde{f}_i$

$$\tilde{f}_i(x, \mu^2) = x f_i(x, \mu^2) \quad . \quad (51)$$



These obey the evolution equations

$$\frac{d \tilde{f}_i(x, \mu^2)}{d \ln \mu^2} = \sum_j \int_x^1 dz P_{ij}(\alpha_s(\mu^2), z) \tilde{f}_j(x/z, \mu^2) . \quad (52)$$

The splitting functions  $P_{ij}$  are computable in QCD perturbation theory as a power series expansion in  $\alpha_s$ :

$$P_{ij}(\alpha_s, z) = \sum_{n=1}^{\infty} \left( \frac{\alpha_s}{2\pi} \right)^n P_{ij}^{(n-1)}(z) . \quad (53)$$

They have the following explicit expressions at leading order:

$$\begin{aligned} P_{gg}^{(0)}(z) &= 2C_A \left[ \left( \frac{1}{1-z} \right)_+ - 1 + \frac{1-z}{z} + z(1-z) \right] + \left( \frac{11}{6} C_A - \frac{2}{3} T_R N_f \right) \delta(1-z) , \\ P_{gq_i}^{(0)}(z) &= P_{g\bar{q}_i}^{(0)}(z) = C_F \frac{1 + (1-z)^2}{z} , \\ P_{q_i g}^{(0)}(z) &= P_{\bar{q}_i g}^{(0)}(z) = T_R \left[ z^2 + (1-z)^2 \right] , \\ P_{q_i q_j}^{(0)}(z) &= P_{\bar{q}_i \bar{q}_j}^{(0)}(z) = C_F \left( \frac{1+z^2}{1-z} \right)_+ \delta_{ij} , \quad P_{q_i \bar{q}_j}^{(0)}(z) = P_{\bar{q}_i q_j}^{(0)}(z) = 0 , \end{aligned} \quad (54)$$

in terms of the  $SU(N_c)$  color factors

$$C_A = N_c , \quad C_F = \frac{N_c^2 - 1}{2N_c} , \quad \text{Tr}(t^a t^b) = \delta_{ab} T_R = \frac{1}{2} \delta_{ab} . \quad (55)$$

### *Flavor structure of the evolution equations*

The leading-order splitting functions  $P_{ab}^{(0)}(z)$  do not depend on the regularization and factorization scheme. This is because they are directly related to observable violation of scaling in deep inelastic scattering. On the contrary, splitting functions and anomalous dimensions beyond leading order do depend on the regularization/factorization scheme. Nonetheless, due to charge conjugation invariance and  $SU(N_f)$  flavor symmetry of QCD, they satisfy the following scheme-independent properties

$$\begin{aligned} \gamma_{q_i g} = \gamma_{\bar{q}_i g} &\equiv \gamma_{qg} , & \gamma_{g q_i} = \gamma_{g \bar{q}_i} &\equiv \gamma_{gq} \\ \gamma_{q_i q_j} = \gamma_{\bar{q}_i \bar{q}_j} &\equiv \gamma_{qq}^{NS} \delta_{ij} + \gamma_{qq}^S , & \gamma_{q_i \bar{q}_j} = \gamma_{\bar{q}_i q_j} &\equiv \gamma_{q\bar{q}}^{NS} \delta_{ij} + \gamma_{q\bar{q}}^S . \end{aligned} \quad (56)$$

The symmetry properties (56) imply that the anomalous dimensions matrix  $\gamma_{ij}$  has only seven independent components. Correspondingly, three flavor non-singlet ( $\tilde{f}^{(V)}$ ,  $\tilde{f}_i^{(-)}$ ,

$\tilde{f}_{q_i}^{(+)}$ ) and two flavor singlet ( $\tilde{f}_S, \tilde{f}_g$ ) parton densities can be introduced so that the evolution equations (52) are completely diagonalized (in the partonic space) for the non-singlet sector. One explicitly finds (we drop the overall dependence on  $N, \mu$  and  $\alpha_s$ )

$$\frac{d \ln \tilde{f}^{(V)}}{d \ln \mu^2} = \gamma^{(V)} \quad , \quad \frac{d \ln \tilde{f}_{q_i}^{(-)}}{d \ln \mu^2} = \gamma^{(-)} \quad , \quad \frac{d \ln \tilde{f}_{q_i}^{(+)}}{d \ln \mu^2} = \gamma^{(+)} \quad , \quad (57)$$

where

$$\tilde{f}^{(V)} \equiv \sum_{j=1}^{N_f} (\tilde{f}_{q_j} - \tilde{f}_{\bar{q}_j}) \quad , \quad \tilde{f}_{q_i}^{(\pm)} \equiv \tilde{f}_{q_i} \pm \tilde{f}_{\bar{q}_i} - \frac{1}{N_f} \sum_{j=1}^{N_f} (\tilde{f}_{q_j} \pm \tilde{f}_{\bar{q}_j}) \quad , \quad (58)$$

and the non-singlet anomalous dimensions are given by

$$\gamma^{(V)} = \gamma_{qq}^{NS} - \gamma_{q\bar{q}}^{NS} + N_f(\gamma_{qq}^S - \gamma_{q\bar{q}}^S) \quad , \quad \gamma^{(\pm)} = \gamma_{qq}^{NS} \pm \gamma_{q\bar{q}}^{NS} \quad . \quad (59)$$

We see from Eq. (54) that all three non-singlet anomalous dimensions are degenerate at one loop. This degeneracy is partially removed at two loops because  $\gamma_{q\bar{q}}^{NS} \neq 0$ . However we still have  $\gamma^{(V)}(\alpha_s) = \gamma^{(-)}(\alpha_s) + O(\alpha_s^3)$  since  $\gamma_{qq}^S$  and  $\gamma_{q\bar{q}}^S$  coincide in  $O(\alpha_s^2)$ . The equality between  $\gamma_{qq}^S$  and  $\gamma_{q\bar{q}}^S$  is violated starting from  $O(\alpha_s^3)$ .

The evolution equations are instead still coupled in the singlet sector:

$$\begin{aligned} \frac{d \tilde{f}_S}{d \ln \mu^2} &= [\gamma_{qq}^{NS} + \gamma_{q\bar{q}}^{NS} + N_f(\gamma_{qq}^S + \gamma_{q\bar{q}}^S)] \tilde{f}_S + 2N_f \gamma_{qg} \tilde{f}_g \quad , \\ \frac{d \tilde{f}_g}{d \ln \mu^2} &= \gamma_{gq} \tilde{f}_S + \gamma_{gg} \tilde{f}_g \quad , \end{aligned} \quad (60)$$

where the quark singlet density is defined by  $\tilde{f}_S = \sum_{i=1}^{N_f} (\tilde{f}_{q_i} + \tilde{f}_{\bar{q}_i})$ .

### 1.2.3 Extensions of the parton picture

We have so far considered the case of scattering from a single incoming hadron. But much of the usefulness and predictive power of the parton picture comes from the fact that it can be extended to a large variety of different processes.

#### *Hadroproduction*

Consider hard production processes in hadron-hadron scattering. The main physical idea in this case is that owing to the Lorentz contraction partons from the two hadrons do not overlap before the hard collision, so that their distributions are not modified by initial-state interactions and stay the same going from deep-inelastic to hadron-hadron

scattering. Factorization formulas for hard cross sections in collisions of two hadrons  $A$  and  $B$  at center-of-mass energy  $s$  have the structure (Fig. 8)

$$\sigma(s, q^2) = \sum_{a,b} \int d\xi_1 d\xi_2 f_{a/A}(\xi_1, \mu_F) f_{b/B}(\xi_2, \mu_F) H_{ab}(\xi_1 \xi_2 s, q^2, \alpha_s(\mu_R), \mu_F) + \mathcal{O}(\Lambda_{\text{QCD}}^2/q^2) \quad , \quad (61)$$

where  $q^2$  is the hard scale,  $H$  is the hard-scattering function, and the  $f$ 's are the parton distributions for the two incoming hadrons. The universality of the  $f$ 's expressed by

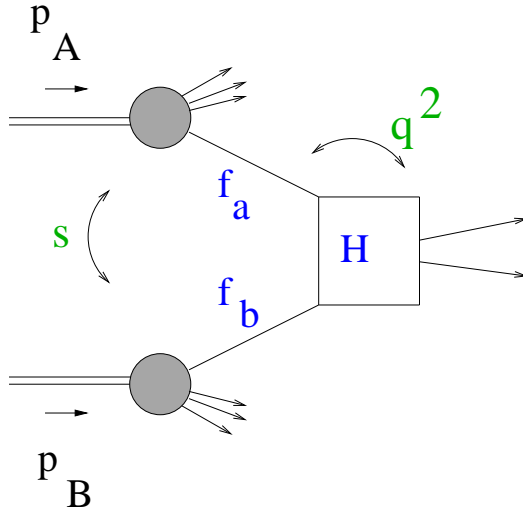


Figure 8: Hard scattering in hadron-hadron collisions.

Eq. (61) allows one to use the  $f$ 's determined from deep-inelastic data to predict different processes such as hadron-hadron collisions. Note that in Eq. (61) we have used a notation that distinguishes between the factorization scale  $\mu_F$  at which the parton distributions are evaluated and the renormalization scale  $\mu_R$  in the coupling. In many applications these scales are identified.

Although the idea behind Eq. (61) is simple, its actual realization is complicated by the intricacies in using arguments based on the Lorentz contraction in the presence of gauge degrees of freedom. This makes detailed derivations rather complex.

### *Fragmentation*

The parton picture has further applications in the case of inclusive hard cross sections that involve the detection of one (or more) hadrons in the final state. In this case factorization formulas are given in terms of nonperturbative distributions  $d_{h/i}(\xi, \mu)$  describing the fragmentation of parton  $i$  into hadron  $h$  as a function of the mass scale  $\mu$  and the fraction

$\xi$  of the parton momentum carried by the produced hadron. These parton fragmentation functions  $d$  are the final-state analogue of the parton distribution functions, and obey evolution equations analogous to Eq. (49) in terms of time-like anomalous dimensions  $\gamma$ ,

$$\frac{d}{d \ln \mu} d_{h/i}(x, \mu) = \sum_j \int_x^1 \frac{d\xi}{\xi} \gamma_{ji}(x/\xi, \alpha_s(\mu)) d_{h/j}(\xi, \mu) . \quad (62)$$

The anomalous dimensions for parton fragmentation functions coincide with those for parton distributions at leading order but differ from them beyond leading order. Like the parton distributions, the functions  $d_{h/i}$  are universal. The same functions appear in cross sections with observed hadrons in hadron-hadron collisions, deep inelastic scattering,  $e^+e^-$  annihilation.